On-land active thrust faults of the Nankai–Suruga subduction zone: The Fujikawa-kako Fault Zone, central Japan

AUTHOR(S):

Lin, Aiming; Iida, Kenta; Tanaka, Hideto

CITATION:

Lin, Aiming ...[et al]. On-land active thrust faults of the Nankai–Suruga subduction zone: The Fujikawa-kako Fault Zone, central Japan. Tectonophysics 2013, 601: 1-19

ISSUE DATE:

2013-08

URL:

http://hdl.handle.net/2433/176993

On-land active thrust faults of the Nankai-Suruga subduction zone: the Fujikawa–kako Fault Zone, central Japan

Aiming Lin[1*], Kenta Iida[2], and Hideto Tanaka[2]

[1]Department of Geophysics, Graduate School of Science

Kyoto University, Kyoto 606-8502, Japan

[2]Graduate School of Science and Technology, Shizuoka Univ.,

Ohya 836, Shizuoka 422-8529, Japan

---

*Corresponding author

Dr. Aiming Lin

Department of Geophysics

Graduate School of Science

Kyoto University

Kyoto 606-8502, Japan

Email: slin@kugi.kyoto-u.ac.jp

Abstract

This paper describes the tectonic topography that characterizes recent thrusting along, the on-land active fault zone of the Nankai-Suruga subduction zone, called the Fujikawa–kako Fault Zone, located near the triple junction of the Eurasian (EUR), Philippine Sea (PHS), and North American (NA) plates, in the western side of Mt. Fuji, central Japan. The analysis was based on interpretations of aerial photographs and 3D perspective images made with Digital Elevation Model (DEM) data, field investigations, and trench excavations. Our study shows the following new observations: 1) distinct east-facing fault scarps are developed on the west-facing slopes, alluvial fans, and terraces of western Mt. Fuji; ii) the total length of the fault zone is ~40 km; iii) the Older stage (ca. 8000–14,000 yr) Fuji lavas have been displaced by as much as 70 m; and iv) the 864–865 AD Jogan lava flow is displaced by 2–4 m vertically along the scarp at the northeastern end of the fault zone. Based on the offsets of lavas and mudflow deposits, as well as historical records, it is found that i) the vertical slip rate for the fault zone is up to

5–8 mm/yr, ii) the recurrence interval of morphogenic earthquakes is estimated to be 150–500 yr, and iii) the most recent seismic faulting event along the Fujikawa–kako Fault Zone is inferred to be related to the 1854 AD (M 8.0–8.5) Ansei–Tokai earthquake.

When compared with the active intraplate faults of Honshu, Japan, the relatively high slip rates and short recurrence intervals for morphogenic earthquakes in the Fujikawa–kako Fault Zone indicate that the activity of this fault zone is closely related to subduction-zone earthquakes and plate convergence near the triple plate junction of the EUR, PHS, and NA plates.

Keywords: Fujikawa-kako Fault Zone, plate boundary, Suruga Trough, active fault, 1854 AD (M 8-8.4) Ansei-Tokai earthquake

1. Introduction

Subduction zones are generally characterized by large earthquakes that contribute about 90% of the total worldwide seismic moment (Uyeda and Kanamori, 1979; Uyeda, 1991), and which can cause great damage from tsunamis, as with the 2004 Sumatra M_w 9.4 and the 2011 M_w 9.0 Tohoku (Japan) earthquakes. The Fujikawa–kako Fault Zone (FKFZ) strikes north–south, and is the inland extension of the Nankai–Suruga Trough where the Philippine Sea (PHS) Plate is being subducted beneath the Eurasian (EUR) Plate (Fig. 1). This subduction zone is a potential source of large subduction-type earthquakes, such as the M ~8 Tokai earthquake in central Japan that has been forecasted for more than three decades (Ishibashi, 1981).

Historical and archeological evidence from the past thirteen centuries point to more than 20 large earthquakes along the Nankai–Suruga and Sagami subduction zones (Ando, 1979; Kondo, 1985; Shiono, 1988; Samgawa, 1992; Seno et al., 1993; Sugiyama, 1994; Kamiichi et al., 2003). The eastern Nankai–Suruga and Sagami troughs experienced a M

7.9 earthquake in 1923, with high-intensity ground motion that was felt throughout the central Japanese island of Honshu, including Tokyo. Based on the historical and seismotectonic data, a major gap in the great interplate earthquakes has been identified in the eastern segment of the Nankai–Suruga Trough, where a M ~8 earthquake is expected to occur in the near future (Ishibashi, 1981). However, the absence of coseismic surface ruptures and any compelling geological evidence for large earthquakes in this gap area has hindered assessment of the long-term behavior of this subduction zone, its associated earthquakes, and seismic hazards for the densely populated Nankai–Suruga coastal region.

Previous studies, based on the analysis of off-fault drilling cores and trench data, and without direct evidence of faulting (Yamazaki, 1992; Yamazaki et al., 2002; The Headquarters for Earthquake Research Promotion, 2010), suggest that the most recent morphogenic faulting event along the Fujikawa–kako Fault Zone occurred at least 1500 years ago. Paleoseismic studies, based on the Holocene sequence from drilling cores in

off-fault areas, suggest six paleoseismic events near the end of the Suruga Trough during the last ~1500 years (Fujiwara et al., 2007; Komatsubara et al., 2007). Topographical evidence and geological investigations revealed the presence of the FKFZ in the southern area of the study region near the Suruga Trough (Tsuya, 1940; Suzuki, 1968; Tsuneishi and Shiosaka, 1981; Tsuchi et al., 1986; Yamazaki, 1992; Yamazaki et al., 2002). However, the fault outcrops along the main trace of the FKFZ lack any evidence of activity over the past 1500 yr, although one trench wall that revealed a faulting event that took place some time before ~2900 yr B.P. (Shimokawa et al., 1996). The deformation features and recent activity of the fault zone remain largely unknown, due to the lack of geological evidence, although a “soon-to-occur large earthquake” (the M ~8 Tokai earthquake) was predicted 30 years ago for the Tokai region, central Japan, around the Suruga Trough (Ishibashi, 1981). Therefore, it is important to understand the seismic potential in this triple plate junction area, and to quantitatively assess the seismic hazard and recent activity of the FKFZ in this densely populated region.

For this study, in order to determine a direct paleoseismic record for the FKFZ, field investigations were conducted as a basis for trench excavations along the fault. This paper reports on the tectonic topographic features along the active faults, and provides evidence that morphogenic earthquakes occurred during the Holocene along the FKFZ in the triple plate junction area along the inland extent of Nankai–Suruga subduction zone.

2. Tectonic Setting

The study region is located along the western foot of Mt. Fuji, a triple plate junction where the PHS Plate is being subducted northwestwards beneath the EUR Plate and north–northeastwards beneath the North American (NA) Plate at a rate of 30–50 mm/yr along the Suruga and Sagami troughs (Fig. 1) (e.g., Kobayashi, 1983; Nakamura, 1983; Seno et al., 1993, 1996; Yamazaki and Seno, 2005). Further to the east on Honshu, the Pacific (PC) Plate is being subducted beneath the NA and PHS plates along the Japan Trench (Fig. 1).

There are many active faults developed along the plate boundaries in the triple plate junction area around Mt. Fuji (Research Group for Active Faults of Japan [RGAFJ], 1991). The FKFZ is one such active fault zone; with a general N–S trend, it dips west, and runs along the inland part of the plate boundary, extending from the Suruga Trough to the triple plate junction with the NA Plate in the northern area (Fig. 1b). On the eastern side of Mt. Fuji, the Kozu–Matsuda Fault Zone (KMFZ) strikes NNW–SSE, dips to the NE, and is an inland extension of the Sagami Trough—the plate boundary between the NA and PHS plates (Fig. 1b). Both the FKFZ and the KMFZ are zones of thrust faulting with high vertical slip rates of up to ~7 mm/yr (RGAFJ, 1991; Yamazaki, 1992) and ~5 mm/yr (Kumaki, 1985; RGAFJ, 1991), respectively. These two fault zones displace the east- and west-facing slopes on the eastern and western foots of Mt. Fuji, forming west- and east-facing fault scarps, respectively (Fig. 1b, c). These distinctive fault scarps mostly face towards the volcanogenic slopes of Mt. Fuji, and the faults offset Holocene volcanic

rocks, including lavas, pyroclastic rocks, and alluvial deposits sourced from Mt. Fuji (Yamazaki et al., 2002).

Historical and archeological evidence points to the probability of at least three M 8 earthquakes at the eastern end of the Suruga Trough in the last millennium: the 1096 Eicho, 1707 Hoei, and 1854 Ansei–Tokai earthquakes, all of which caused great damage over a wide area around central–western Japan, with seismic intensities estimated to have been VI–VII (Japanese standard with a maximum intensity VII) (Usami, 1975). Recently, a M_w 6.4 earthquake occurred on 15 March 2011, ~3 km east of the FKFZ (Fig. 1), and it is thought to have been triggered by the drastic change of crustal stress caused by the M_w 9.0 Tohoku (Japan) earthquake of 11 March 2011 in east–northeastern Japan (Geospatial Information Authority of Japan, 2011).

We undertook field investigations immediately after the 11 March 2011 earthquake, but found no obvious surface rupturing in the epicentral area around the FKFZ. However, the high seismic activity in this triple plate junction area shows that these active faults are

potentially seismogenic.

3. Topographic Features and Geological Structures of Active Faults

3.1. Study methods

Since the crustal deformation associated with active faults and folds is generally preserved in current landforms, and characterized by displaced topographic markers such as terraces, alluvial fans, ranges, and valleys, it is possible to recognize and identify active faults and fault-related folds by studying tectonic-related topographic surface features (e.g., Yeats et al., 1997; Lin et al., 2008). It is well known that tectonic-related topographic features that develop around active faults and folds record displacements during large-magnitude earthquakes (e.g., RGAFJ, 1991; Yeats et al., 1997; Lin et al., 2009), and that tectonic-related topographic studies are essential for developing a historic and/or paleoseismic perspective of the locations, magnitudes, recurrence intervals, and slip patterns of seismogenic faults.

In order to detect and identify tectonic topographic features associated with active faults and flexural fold structures in the study area, we examined aerial-photos, used color-shaded relief maps generated by 1/25,000 DEM data with 10 m mesh grids released by the Geospatial Information Authority of Japan (2012). On the perspective images, to emphasis and silhouette the visible fault scarps that strike north–south and face east, the rays of the sun were placed coming from the west so the scarps are in shade (Figs 2 and 3). These methods made it possible to identify tectonic-related topographic features in vegetated areas of the study area (Figs 1 and 2a). The presence of faults, identified by these methods, was confirmed in the field by trench excavations and the digging up of outcrops along the probable fault traces.

The results show that the FKFZ consists of several parallel to subparallel active faults and fault-related flexural fold structures, with a complex geometry of fault traces that extend for ~40 km in length and form a fault zone of 2–5 km in width, generally <4 km (Fig. 2b). Topographically, these faults displace the west-facing slope of Mt. Fuji, and

form east-facing fault scarps along the western foot of the mountain (Fig. 2a). Based on the topography, fault geometry, and geological structures, the FKFZ can be divided into three segments: southern, central, and northern. These are described below in detail (Fig. 2b).

3.2. Southern segment

The southern segment of the FKFZ, located in the southwestern foot of Mt. Fuji, consists mainly of three faults: the Iriyama and the Iriyamase faults that strike north–south, and the Omiya Fault that strikes northwest–southeast (Fig. 3). The Iriyama and the Iriyamase faults are bounded on the northern end by the Omiya Fault and extend southwards into the Suruga Trough. Previous studies have provided topographical and geological evidence for the active faults of this segment (Fig. 3; Tsuya, 1940; Suzuki, 1968; Tsuneishi and Shiosaka, 1981; Tsuchi et al., 1986; Yamazaki, 1992; Yamazaki et al., 2002). Here, we describe the main topographical and geological characteristics of these

active faults by comparing the results of previous workers with data of the present study, which include the interpretative results of analyses of aerial photographs and perspective view images.

3.2.1. Iriyama Fault

The main trace of the Iriyama Fault follows a north–south striking valley in an intermontane area made up of Tertiary–Pleistocene sedimentary rocks (Tsuchi et al., 1986). Where the fault trace cuts across the northeast–southwest striking range, it forms a distinct linear feature that extends to the east-facing scarp of the Suruga Trough in the south (Fig. 3a, b). The deformational features and recent activity of the Iriyama Fault are still unclear due to a lack of distinct evidence for displacement of Holocene topographic markers such as terraces and alluvial fans and fault structural features.

3.2.2. Iriyamase Fault

The Iriyamase Fault is developed at the southeastern end of Hoshiyama Hill, and it extends southwards through the channel of the Fujikawa (Fuji River) into the Suruga Trough (Fig.3; Yamazaki, 1992). It branches into two subfaults in the northern segment: one forms the boundary between Hoshiyama Hill and the Holocene lowlands to the southeast (Fig. 3b), and the other cuts Hoshiyama Hill along a straight valley (Figs. 3a, d, and 4). The branch cutting Hoshiyama Hill was discovered during the present study, and is named the Iwamoto Fault. The Iriyamase Fault in the southern segment is covered by current Fuji River channel deposits consisting of sand-gravel and volcanic rocks, and no obvious tectonic features can be recognized on the surface. Drilling data from both sides of the fault show that Older stage lavas (8000–14,000 yr) from Fuji volcano, and sediments containing peat layers (8000 yr), have been offset vertically by approximately 105 m and 46 m, respectively (Yamazaki, 1992). Based on these displacements of the lava and peats, the vertical slip rate of the Iriyamase Fault is estimated to be ~5–7 mm/yr

(Yamazaki, 1992).

A topographical map published in 1888 AD (20th year of the Meiji Dynasty) (Tsuneishi and Shiosaka, 1981; RGAFJ, 1991) shows co-seismic surface ruptures produced by the 1854 M 8.4 Ansei–Tokai earthquake, and these ruptures occur close to the inferred trace of the Iriyamase Fault (Fig. 3b). These surface ruptures are mainly characterized by co-seismic push-up structures that form two small, narrow hills of 1-2m in height [called the Earthquake Mountains in Japan (Tsuneishi and Shiosaka, 1981; RGAFJ, 1991)], parallel to the fault trace on the lowlands and lowest terraces of the Fuji River (Fig. 3a, b). The occurrence of these co-seismic surface features indicates that the Iriyamase Fault may have been a source seismogenic fault of the 1854 AD (M 8-8.4) Ansei–Tokai earthquake (see Discussion below for further details). The inferred fault trace extends southwards to the Suruga Trough (Fig. 3).

One typical fault outcrop of the Iwamoto Fault was observed on Hoshiyama Hill, where the fault separates unconsolidated sand–gravel layers in the footwall from

silt-mudstone in the hanging wall at a high angle of 75° (Fig. 4). Some silt–sand veins with an irregular geometry were injected into the silt-mudstone within a narrow zone less than 1 m from the main fault plane, and the veins themselves are offset by subfaults or fractures (Fig. 4c, d). These injection veins are considered to have formed during liquefaction of the unconsolidated silt–sands during large paleo-earthquakes, and to have been offset by subsequent seismic faulting events. The striations and fault steps on the main fault plane show a thrust-dominated movement sense (Fig. 4 b, e), coincident with that of the vertical offset of Hoshiyama Hill (Fig. 4b). These fault-related structures and liquefaction of slit-sands indicate that repeated large paleo-earthquakes have taken place along this fault.

3.2.3. Omiya Fault

The Omiya Fault strikes northwest–southeast, and forms a sharp scarp that faces northeast between Hoshiyama Hill (Hy-hill) and the Fujinomiya Holocene lowlands that

are tilted to the southwest (Fig. 3a, b). A new highway (2nd Tomei Highway), opened in April 2012, crosses the fault scarp, which is a matter of serious concern in terms of seismic hazards (Fig. 5). This fault was first inferred to be active by Tsuya (1940), and this was subsequently confirmed by trench investigations (Shimokawa et al., 1996). The perspective topographical image of the fault trace shows a distinct and straight linear feature in its southeastern part (Fig. 3). Hoshiyama Hill is mainly made up of volcanic rocks (the Older stage lava) and mudflow deposits (Ko–Fuji mudflow) (~10,000–100,000 yr) from Mt. Fuji (Fig. 3b; Yamazaki, 1979; Tsuchi et al., 1986) that originally formed a continuous slope towards the southwest from Fuji volcano, but which now is folded and offset vertically by ~100 m (Figs 3b, d, and 5a). The flexural fold structures within the Holocene deposits including volcanic rocks and unconsolidated mudflow and the flexural morphology of topographical surface are constrained in a narrow zone of <500 m in the uplift side (hanging wall) of the fault and the axes of flexural fold structures are oriented to parallel-subparallel to the Omiya Fault (Figs 3b, d, and 5a). The parallel-subparallel

orientation of the flexural fold axis and fault traces is also observed in the central segment (Fig. 6b), indicating a thrusting-related formation mechanism. Topographical profiles show that Hoshiyama Hill is offset vertically by at least 94–137 m (Fig. 3c-e). Geological data including field works and drilling data on the both sides of the Omiya Fault also shows that the Pleistocene basement rocks including sedimentary and volcanic rocks are offset vertically by 80–130 m (Yamazaki, 1992; Yamazaki et al., 2002). Based on topographical and drilling data, as well as ^{14}C dating, the average vertical slip rate is estimated to be ~2–4 mm/yr (Yamazaki, 1992; Yamazaki et al., 2002).

3.3. Central segment

The central segment contains the Agoyama, Kubo, Shibakawa, Saori, and Kamiide faults, all of which generally strike north–south, and are accompanied by flexural fold structures with axes generally striking north–south to northeast-southwest. These faults form a zone approximately ~4 km wide (Figs 6 and 7). The Agoyama and Shibakawa

faults have been mapped previously (RGAFJ, 1991; Yamazaki, 1992; Nakada et al., 2002; Yamazaki et al., 2002; Maruyama and Saito, 2007), but the Kubo, Saori, and Kamiide faults, and the related flexural fold structures in the northern part of this segment, were discovered during the present study. Topographical surfaces around this fault zone are strongly deformed and offset, and parallel–subparallel flexural fold structures are well developed, which are constrained in the limited areas within the fault zone (Figs 6 and 7). The fold axes of flexural fold structures are oriented to parallel to subparallel to the main fault traces of the Agoyama, Shibakawa, and Kamiide faults (Fig. 6b), as those observed in the southern segment (Figs 3b and 5a). The Habuna and Shibakawa hills, which run north–south, are bound by the Agoyama and Kamiide faults to the east and the Shibakawa and Saori faults to the west.

3.3.1. Agoyama and Kamiide faults

As shown in Fig. 6, the Agoyama and Kamiide faults present a series of

discontinuous but distinct fault scarps, generally facing east against the west-facing volcanic slope of Mt. Fuji. These scarps form the boundary between the Habuna–Shibakawa hills and the slope of Mt. Fuji. Topographic profiles show that the height of the Agoyama fault scarp is up to ~170 m, and drilling data reveals that the Ko-Fuji mudflow is offset vertically by ~410 m (Fig. 6c). The eastern side of the fault scarp is covered by Holocene alluvial deposits, and here, no outcrop of the fault can be found along its trace. Based on the vertical offset amount of the Ko–Fuji mudflow (ca. 80,000 yr B.P.), the vertical slip rate is estimated to be ~5 mm/yr (Yamazaki, 1992).

3.3.2. Shibakawa, Kubo, and Saori faults

The Shibakawa, Kubo, and Saori faults are developed along the boundary between the mountains in the west and the Habuna–Shibakawa hills where the Ko-Fuji mudflow and Old stage lava are distributed (Figs. 5 and 6). The scarps of the Shibakawa, Saori, and Kamiide faults developed within the Old stage lava are 79–85 m in height (Fig. 6e–f),

lower than the Agoyama fault scarp (Fig. 6c). The Kubo Fault is developed along the western side of Habuna Hill, and its scarp faces west, forming a narrow graben structure on the east-facing scarp of the Shibakawa Fault (Figs 6 and 7). Many outcrops of the Shibakawa, Kubo, Saori, and Kamiide faults were observed in the field, and five typical exposures (Locs 3–7) that show Holocene activity are described below (Figs 8–13).

Outcrops of the Shibakawa Fault can be observed at Locs 3 and 4 (Figs 8–10). At Loc. 3, on a fault scarp (Fig. 8), Holocene deposits (mainly unconsolidated to weakly consolidated silt–sand, loam, and pumice) are offset by faulting. Sand boil structures occur within the medium-grained sand layer at the bottom of the exposure wall, indicating liquefaction at this location; these liquefaction structures were then cut and offset by later faults and many fractures (Fig. 8). Dating of the organic soils in these deposits yields ^{14}C ages of 5381–9488 yr B.P. (Fig. 8b; Table 1). These ^{14}C ages, and the fault and liquefaction structures which were cut and offset by faults and fractures subsequently, indicate repeated seismic events along the Shibakawa Fault during the

Holocene.

Two sets of trench excavations were carried out at Loc. 4, where two parallel fault scarps are developed on a young alluvial fan (Figs 9 and 10). All alluvial layers, except the current surface soil, have been deformed and displaced by the faults. Radiocarbon dating shows that the humic soil layer in the upper part of the exposure wall formed during the past ~600–1300 years (Figs 9 and 10; Table 1). The ^{14}C ages and the fault displacement structures, indicate at least one recent seismic event on the Shibakawa Fault during the past 600–1300 years (see Discussion below for more details).

A large cutting of ~15 m long, on the ~1.3 m high west-facing scarp of the Kubo Fault, was exposed during road construction at Loc. 5 (Fig. 11). To examine the fault structures here, I re-trenched and smoothed the exposure wall (Fig. 11). The outcropping deposits are mainly composed of soils and loams sourced from the volcanic rocks of Mt. Fuji, including ash, pumice, and scoria, with the organic soils sourced from surface vegetation. Radiocarbon dating shows that the upper part of the exposure, down to about

3 m, formed in the past 3000–4000 years, and that the uppermost layer (surface soil) formed in the past ~1500 years (Fig. 11; Table 1). The Shibakawa lava (ca. 14,000 yr B.P; Yamamoto et al., 2007) is exposed at the bottom of the exposure. Sand boil structures are observed in a layer of pumiceous humic soil, bounded below by a layer of silt. All the layers in the deposit are displaced. In contrast with the 1.3 m high fault scarp, the yellowish loam layer shows a displacement of ~8 m along the main fault plane during the late Holocene (Fig. 11). This means that the amount of displacement was gradually accumulating along the main fault plane. Based on ^{14}C dating and offsets of the surface soil layer, it is inferred that the most recent seismic event occurred during the past ~1500 years (see Discussion below for more details).

The scarp of the Kubo Fault and associated structures can also be observed at Loc. 6 (a Jomon-period archeological excavation site) at ~50 m north of Loc. 5 (Fig. 12). All the layers in the exposed deposits, except the surface soil layer, have been cut and deformed by faults. Radiocarbon dating shows that the deposits are sourced from

volcanic rocks that formed in the past ca.1100–4000 years (sample nos. FK-8 and FK-9) including scoria and pumice (Fig. 12; Table 1). The structures and ^{14}C dating indicate a recent seismic event on the Kubo Fault in the past 1100 years, consistent with the conclusions reached at Locs 4 and 5, as discussed above (also see the Discussion section below for further details).

A fault outcrop is exposed in a small stream channel at Loc. 7 on the scarp of the Saori Fault (Fig. 13). Here the fault separates consolidated Ko–Fuji mudflow and weakly-consolidated to unconsolidated mudflow made up of mud, sand, and coarse gravels . A piece of wood from the consolidated Ko–Fuji mudflow yields a ^{14}C age of 23,400 yr (Fig. 13; Table 1), indicating that consolidated and weakly consolidated mudflows, formed in the past 23,400 years, have been displaced by the fault, demonstrating recent activity along the Saori Fault and its scarp.

Structures related to the Kamiide Fault were observed on its high scarp at a construction site for a dam at Loc. 8 (Figs 6f and 14). The new stage Fuji lava, which

flowed from Mt. Fuji on the eastern–southeastern side of Loc. 8, formed a west–northwestwards sloping surface which was then uplifted and tilted to the east–northeast (Fig. 14a, b). The surface soil on a mudflow deposit, made up of volcanic rock debris, was burned, and is now brown in color (Fig. 14b). The structures are exposed at the foot of the fault scarp in a large wall more than 30 m long (Fig. 14c). Here, the alluvial deposits, made up of silt–sand, gravel, and volcanic ash (including pumice and scoria), are folded and displaced to form a graben structure (Fig. 14c–e). Radiocarbon dating shows that the alluvial deposits that contain scoria and pumice formed during the period BC 100–2300, and that the youngest sand–gravel formed in the past 1300 yr (647–686 AD) (Fig. 14e; Table 1). This youngest sand–gravel also indicates a recent seismic faulting event in the past 1300 yr, consistent with the event inferred from the fault scarp developed on the Aokigahara lava, as mentioned above.

In summary, field investigations and ^{14}C dating show that the faults in the central segment were active in the late Holocene, and that the most recent faulting occurred

during the past 600–1300 yr. On the basis of the amount of vertical offset (79–85 m) of the Older stage lava (8–11 ka) (Fig. 6b, d, e), the vertical slip rate is estimated to be 6–10 mm/yr, with an average of 8 mm/yr.

3.4. Northern segment

The main fault in the northern segment of the FKFZ is the Omuroyama Fault, which strikes northeast–southwest and extends to the western side of the Omuroyama Volcano (Fig. 15). The fault cuts all Holocene volcanic rocks on the northwestern slope of Mt. Fuji, including the Aokigahara lava (New stage lava) that formed during the 864–865 AD Jorgan eruption of Fuji (Tsuya, 1968) (Figs 1 and 15b). Its scarp reaches heights of 28–55 m on the surface of the new stage Fuji lava (<11,000 yr B.P.; Tsuya, 1968; Miyachi et al., 1992) in its southwestern part (Figs 15c, d, and 16a), and decreases gradually in size to a height of 2–3 m at its northeastern end where it cuts the surface of the Aokigahara lava that erupted during the Jogan eruption (864 AD) (Figs 15e, f, and

16b). This relatively low fault scarp on the Aokikahara lava indicates at least one morphologic earthquake has occurred since the formation of the Jogan lava, during the last millennium (see Discussion below for further details). Based on the vertical offset of the Older stage lavas, the vertical slip rate of this fault is estimated to be 4–7 mm/yr, comparable to the slip rate in the southern segment of the FKFZ, as noted above.

4. Discussion

4.1. Total length of the FKFZ

The length of fault ruptures produced by large, individual earthquakes, is a key parameter in assessing the seismic moment, the rupture mechanism, the degree of seismic hazard, and the activity of a seismogenic fault, including the recurrence interval for large earthquakes, and the long-term slip rate (e.g., Yeats et al., 1997; Lin et al., 2001, 2009). The length of an active fault zone is usually used as a factor in assessing the potential magnitude of future earthquakes generated on the fault (Matsuda, 1975). Based on the

width of coseismic surface zone reported in the world, a total width of up to 5 km is also used as a critical distance for grouping active faults as a seismogenic fault zone (Matsuda, 1990). The FKFZ is one of the most active of fault zones, and it has the potential to trigger a strong earthquake in the near future in Japan. For these reasons, the FKFZ has been chosen for special earthquake observation and hazard assessment (The Headquarters for Earthquake Research Promotion, 1998, 2010). On the basis of topographical and geological investigations, including drilling and geophysical observations over the past two decades, previous studies indicated that the total length of this fault zone is ~26 km (Yamazaki et al., 2002; Maruyama and Saito, 2007; The Headquarters for Earthquake Research Promotion, 2010). Based on its length and tectonic setting, the FKFZ is considered to be a continental extension of the seismogenic fault that is linked to the subduction zone along the Suruga Trough, and which will trigger the projected M ~8 (± 0.5) Tokai earthquake. However, it has not been assessed as a seismogenic fault capable of triggering a M ~8 earthquake (The Headquarters for Earthquake Research Promotion,

2010). On the other hand, Tanaka et al. (2003) reported that the total length of the FKFZ is >35 km, based on field investigations and trench excavations. During this present study, good topographical and geological evidence was found to show the FKFZ extends northwards near the Omuroyama Volcano for approximately 40 km with general width of <4 km, as noted above. Based on the relationship between the lengths (L) of active faults and the width of seismogenic fault zone in Japan and earthquake magnitudes (Log L = 0.6M – 2.9; Matsuda, 1975, 1990), the FKFZ can therefore be regarded as an independent seismogenic fault with the potential to produce an earthquake of M 7.5. If the FKFZ is linked with the subduction thrust zone along the Suruga Trough, it then becomes possible to trigger a M ~9 subduction-type earthquake, similar to the 2011 Tohoku (Japan) earthquake along the FKFZ–Suruga Trough. Our results show that it is necessary to reassess the nature of seismic hazard of the FKFZ for densely populated central Japan, based on the new findings presented in this study.

4.2. Timing of the most recent large earthquake on the FKFZ

Timing of the most recent morphological earthquake is a key factor for earthquake forecast and for assessing the seismic hazard in an active fault region. The current theoretical basis for long-term earthquake forecast is based on the recurrence interval of morphological earthquakes and the time that has elapsed since the most recent large earthquake in that region (Matsuda, 1975; RGAFJ, 1991). The trench excavations, field investigations, and ^{14}C dating of the present study, as described above, show that the most recent morphogenic earthquake on the FKFZ, producing surface rupture, occurred during the past 500–800 years (Figs 9 and 10), after the 864 AD Jogan eruption from Fuji volcano. Historical records document two large earthquakes of M ~8 (± 0.5) that caused great damage in the Tokai region and around the study area in the past 800 years: the1707 Hoei and the 1854 Ansei–Tokai earthquakes (Usami, 1975; Utsu et al., 1987). The 1707 Hoei earthquake caused widespread damage in central Honshu, and it produced strong ground motion with seismic intensity VI–VII (the strongest seismic intensity of the 0–VII

classes used in Japan) in the coastal region from Shikoku Island to the Tokai region, around the study area, and parallel to the Nankai–Suruga Trough. This earthquake originated in the subduction zone, and rupturing occurred along the Nankai–Suruga Trough for >500 km (Koyama, 2007), comparable to the 2011 M_w 9.0 Tohoku (Japan) earthquake. Following the 1707 Hoei earthquake, Mt. Fuji erupted on 16 Dec. 1707, 49 days after the main shock (Koyama, 2007). Based on historical records in the temples and shrines around the study region, it is inferred that co-seismic rupturing did not occur in the coastal region around the Suruga Trough (Nakanishi and Yano, 1998). The geographical maps made during 1699–1743 AD also show no evidence of ground deformation in the coastal area around the Suruga Trough, due to the Hoei earthquake (Fujiwara et al., 2011). These records show that the Fujikawa–kako Fault did not rupture during the 1707 Hoei earthquake.

The 1854 Ansei–Tokai earthquake in the Tokai region caused strong ground motions of seismic intensity VI–VII in a limited area along the Fujikawa–kako Fault and

the coastal area around Suruga Bay (Usami, 1975). Historical records show that i) liquefaction occurred in a narrow zone around the FKFZ that extended to the Kofu basin in the north, and in this zone ~70% of buildings were completely destroyed (Utsu et al., 1987); ii) 4–6 m high tsunami run-ups occurred along the Tokai coastal region around the Suruga Trough; and iii) the ground along the coastal region around Suruga Bay was uplifted 1–2 m, and two push-up structures in limited areas within the southern segment of the FKFZ were uplifted 1-2 m as small hills, which are push-up structures appropriately called the Earthquake Mountains in Japan (Fig. 3b) (RGAFJ, 1991). One day after the Ansei–Tokai earthquake, the M ~8 Ansei–Nankai earthquake occurred in the Naikai Trough, and this also caused great damage and generated tsunamis in central Japan. Historical documents show that the epicenter of the 1854 Ansei–Tokai earthquake was located in the area around the FKFZ and the Suruga Trough. The results of trench and field investigations, as described above, show that at least one morphogenic earthquake has occurred in the past 600–800 years, displacing the alluvial deposits that

formed during the past 1000 years, and the 864 AD Jogan lava. On the basis of the historical documents and geological evidence, as documented above, we conclude that the most recent morphogenic earthquake on the FKFZ may correspond to the 1854 Ansei–Tokai earthquake. In other words, the FKFZ is a potential seismogenic fault that probably triggered the 1854 M ~8 Ansei–Tokai earthquake.

4.3. Slip rates and recurrence intervals of morphogenic earthquakes

The long-term slip rates of active faults are generally determined by observing the displacements of topographical and stratigraphic markers of relatively recent and known age. In the study area, the widely distributed volcanic rocks that came from Fuji, including lava, mudflow deposits, pumice, and scoria, are used as markers to determine the slip rate of the FKFZ (Yamazaki, 1992; Yamazaki et al., 2002). In the southern and central segments of the FKFZ, the average vertical slip rate is estimated to be up to a maximum of ~5–8 mm/yr, based on the displacements of alluvial deposits and the

Pleistocene volcanic ashes and Ko–Fuji mudflow in the Habuna–Hoshiyama hills (e.g., Yamazaki et al., 1979; RGAFJ, 1991; Yamazaki, 1992). In the northern segment, the widely distributed Holocene volcanic rocks are used as markers to calculate the slip rate. As shown in Figs 2b and 13, the Holocene lavas (<11,000 yr B.P.) are offset vertically by ~55 m, and the vertical slip rate is therefore calculated to be ~5 mm/yr, comparable with the rate in the southern and central segments.

The recurrence intervals of morphological earthquakes are generally inferred from historical records and paleoseismic data. As described above, the heights of fault scarps produced by the most recent faulting event along the FKFZ are as follows: 1.3–1.5 m on the Shibakawa Fault in the central segment (Fig. 10), 2.5–3.0 m on the Omuroyama Fault in the northern segment, and 1–2 m uplift in the southern segment, as indicated by the Earthquake Mountains along the Iriyamase Fault. Based on the heights of these fault scarps, and ground uplift caused by the 1854 earthquake, we conclude that the characteristic vertical offset that resulted from the 1854 Ansei–Tokai earthquake is on

average 1–3 m, comparable with the 1–3 m vertical offset caused by the 2011 M_w 7.9 Wenchuan earthquake along the Longmen Shan Thrust Belt (Lin et al., 2009, 2012). Using these offset amounts, and a slip rate of 5–8 m/ka, the recurrence interval for the FKFZ is calculated to be ~150–500 years. This contrasts with the previous estimates of 1300–1600 years (The Headquarters for Earthquake Research Promotion, 2010), but is comparable with the 150–300 years inferred from studies of the off-fault deformation of sediments (Fujiwara et al., 2007). A shorter recurrence interval of ~150–500 years clearly necessitates a major revision of the existing seismic-hazard model for the densely populated Tokai region of Japan.

The recurrence interval calculated for the FKFZ in the present study is much shorter than the recurrence intervals for the main intracontinental active faults in Japan, which are ~1000 to more than 10,000 years, and typically 2000–4000 years (RGAFJ, 1991). However, the figure for the FKFZ is comparable to the ~50–400 years recurrence interval for subduction-zone earthquakes along the Suruga–Nankai and Sagami troughs

(The Headquarters for Earthquake Research Promotion, 2010). These findings lead to the conclusion that the FKFZ is an inland extension of the active fault developed on the subduction zone along the Suruga Trough.

5. Conclusions

On the basis of the field and trench investigations described above, and the ensuing discussion, the following conclusions have been reached regarding the nature and activity of the FKFZ.

1) The total length of the fault zone is ~40 km, and it is an inland extension of the active fault developed in the subduction zone along the Suruga Trough.

2) The vertical slip rate is calculated to be up to ~5–8 mm/yr.

3) The most recent morphogenic earthquake on the FKFZ corresponds to the 1854 AD (M ~8) Ansei–Tokai earthquake.

4) The recurrence interval of morphogenic earthquakes on the FKFZ is estimated to be ~150–500 years. This is much shorter that the recurrence interval for the

main intracontinental active faults of Japan, but it is comparable with the interval for subduction-zone earthquakes.

Acknowledgments

We thank T. Maruyama, J. Shin, J. Guo, G. Rao, and B. Yan, for their assistance in the field and landowners K. Ashikawa and S. Kano for their kind permission and help in excavating the trenches. We are grateful to two anonymous reviewers for critical reviews that helped to improve the manuscript. This work was supported by a Grant-in-Aid for Scientific Research (A) (Science Project No. 23253002) for A. Lin from the Ministry of Education, Culture, Sports, Science, and Technology of Japan.

References

Ando, M., 1975. Source mechanisms and tectonic significance of historical earthquakes along the Nankai trough, Japan, Tectonophysics 27, 119–140.

Fujiwara, O., Sawa, Y., Morita, Y., Komatsubara, J., Abe, K., 2007. Coseismic subsidence recorded in the Holocene sequence in the Ukishima-ka-hara, Shizuoka Prefecture, central Japan. Annual Report on Active Fault and Paleoearthquake Researches 7, 91–118.

Fujiwara, O., Yada, T., Shisikura, M., 2011. Change in the coastal line around the Makiharashi region before and after the Hoei earthquake, inferred from the historical topographic maps. Abstract, Annual Meeting, The Society of Historical Earthquake Studies, Niigata, Sep. 16, 2011 (in Japanese).

Geological Survey of Japan, 2002. Geological map of Shizuoka region. Ibaraki, Japan, Geol. Surv. Jpn, scale 1:200,000.

Geospatial Information Authority of Japan, 2012. Maps & Geospatial Information.

http://www.gsi.go.jp/ENGLISH/page_e30031.html (last accessed 30 Oct, 2012).

Ishibashi, K., 1981. Specification of a soon-to-occur seismic faulting in the Tokai district, central Japan, based upon seismotectonics. Earthquake Prediction-An International Review. Maurice Ewing Series 4, Am. Geophys. Union 297–332.

Japan Meteorological Agency, 2011. Earthquake information. http://www.jma.go.jp/jma/indexe.html (last accessed 20 March, 2013)

Kamiichi, M., Lin, A., 2003. Late Quaternary activity of active faults in the Udo Hill, Shizuoka Prefecture. Active Fault Research 23, 45–52.

Kobayashi, Y., 1983. Initiation of subduction of a plate. Earth Month 5, 510–514 (in Japanese).

Komatsubara, J., Shishikura, M., Okamura, Y., 2007. Activity of Fujikawa-kako fault zone inferred from submergence history of Uskishima-ga-hara lowland, central Japan. Annual Report on Active Fault and Paleoearthquake Researches 7, 119–128.

Koyama, M., 2007. 1707 eruption and change process of Mt Fuji. Zisin Journal 44, 8-15 (in Japanese).

Kumaki, Y., 1985. The deformation of Holocene marine terraces in southern Kanto, central Japan. Geogr. Rev., Japan 50B, 49–60.

Lin, A., Ren, Z., Jia D., Wu, X., 2009. Co-seismic thrusting rupture and slip distribution produced by the 2008 M_w7.9 Wenchuan earthquake, China. Tectonophysics 471, 203–215, DOI:10.1016/j.tecto.2009.02.014

Lin, A., Rao, G., Yan, Y., 2012. Field evidence of rupture of the Qingchuan Fault during the 2008 M_w7.9 Wenchuan earthquake, northeastern segment of the Longmen Shan Thrust Belt, China. Tectonophysics 522-523, 243–252, doi:10.1016/j.tecto.2011.12.012.

Lin, A., Kano, K., Guo, J., Maruyama, T., 2008. Late Quaternary activity and dextral strike-slip movement on the Karakax Fault Zone, northwest Tibet. Tectonophysics 453, 44–62, doi:10.1016/j.tecto.2007.04.013.

Maruyama, T., Saito, M., 2007. Geological survey on the activity and recurrent history of large earthquakes of the Fujikawa-kako Fault Zone. Result report on “Additional and complementary investigations of the fault zones for basic observation and investigation”, No.H18-4, pp.39, National Institute of Advanced Industrial Science and Technology, Japan.

Matsuda, T., 1975. Magnitude and recurrence interval of earthquake from a fault. Zisin, Journal of Seismological Society of Japan 28, 269–283 (in Japanese with English abstract).

Matsuda, T., 1990. Seismic zoning map of Japanese Islands, with Maximum magnitudes derived from active faults data. Bull. Earthq. Inst., Univ. Tokyo 69, 289–319.

Miyachi, N., Endo, K., Togashi, S., Uesugi, Y., 1992. Tephronological history of Mt. Fuji. 29th IGC Field trip C12.

http://www.geo.chs.nihon-u.ac.jp/quart/fuji-p/dgi-rts-f/chisitsu-p.html (last accessed 30 Oct. 2012)

Nakata, T., Togo, M., Ikeda, Y., Imaizumi, T., Une, H., 2002. Active faults in urban area, Fujinomiya, 1:25,000, Graphical Survey Institute, Japan.

Nakamura, K., 1983. Possibility of a nascent plate boundary at the eastern margin of the Japan Sea (in Japanese). Bull. Earthquake Res. Inst., Univ., Tokyo, 58, 711–722.

Nakanishi, I., Yano, M., 2005. Location of eastern end of source area of the 1707 Hoei earthquake. Geophysical Bulletin of Hokkaido University, Japan, 68, 255-259.

Research Group for Active Faults of Japan (RGAFJ), 1991. Active Faults in Japan-Sheet maps and inventories. University of Tokyo Press, pp.437.

Sangawa, A., 1992. Earthquake Archeology, Chuko Shinsho, 251p, Tokyo (in Japanese).

Seno, T., Stein, S., Griff, A.E., 1993. A model for the motion of the Philippine Sea plate consistent with NUVEL-1 and geological data, J. Geophys. Res. 98, 17941–17948.

Seno, T., Sakurai, T., Stein, S., 1996. Can the Okhotsk plate be discriminated from the North American plate? J. Geophys. Res. 101, 11305–11315.

Shimokawa, K., Yamazaki, H., Mizuno, K., Tanaka, R., 1996. Paleoseismology and active fault study of the Fujikawa fault system. In: 1995 Summary report of the active fault survey. GJS Openfile reports No.259, 73–80 in Japanese).

Shiono, K., 1998. Seismicity of the SW Japan arc-subduction of the young Shikoku basin, Modern Geology 12, 449–464.

Suzuki, T., 1968. Settlement of volcanic cones. Bull. Volcano. Soc. Japan 13, 95–108.

Stuiver, M., Reimer, P.J, Reimer, R., 2003. CALIB Radiocarbon Calibration Version 4.4. http://radiocarbon. pa.qub.ac.uk/calib/. Last accessed, 20 March 2013).

Tanaka, H., Lin, A., Maruyama, T., 2003. Abstract, Japan Geoscience Union Meeting, 2003, Chiba, Japan.

The Headquarters for Earthquake Research Promotion, 1998. Assessment and investigation results of the Fujikawa-kako Fault Zone. http://www.jishin.go.jp/main/chousa/fujikawa/ (last accessed 30 Oct. 2012)

The Headquarters for Earthquake Research Promotion, 2010. Re-evaluation of the

Fujikawa-kako fault zone. 54p.

http://www.ipc.shizuoka.ac.jp/%7eslin/english.html (last accessed 30 Oct 2012)

Tsuchi, T., Kuroda, N., Kano, K., Ibaraki, M., 1986. Geological map of the Shizuoka Prefecture, 1:200,000. Naigai Map Co. Ltd, Tokyo.

Tsuneishi, Y., Shiosaka, K., 1981. Fujikawa Fault and Tokai Earthquake. Journal of the Japan Society of Engineering Geology 23, 52–66.

Tsuya, H., 1940. Geology and petrological studies of volcano Huzi (Fuji), III. Bull. Earthq. Res. Inst. 18, 419–445.

Tsuya, H., 1968. Geological map of Mt. Fuji, 1:50,000. Geological Survey of Japan.

Usami, T., 1975. Catalog of damaged earthquakes in Japan. Tokyo University Press, Tokyo.

Utsu, T., Shima, E., Yoshii, T., Yamashina, K., 1987. Encyclopedia of Earthquake. Pp.568, Asagura Shoden Ltd., Tokyo.

Uyeda, S., 1991, The Japanese island arc and the subduction process, Episodes, 14,

190–198.

Uyeda, S., Kanamori, H., 1979. Back-arc opening and mode of subduction, J. Geophys. Res. 84, 1049–1061.

Yamamoto, T., Ishizuka, Y., Takada, A., 2007. Surface and subsurface geology at the southwestern foot of Fuji volcano, Japan: new stratigraphy and chemical variation of the products. in: “Fuji volcano” (edited by Fujii, T. et al.), 97–118 (in Japanese)..

Yamazaki, H., 1979. Active faults along the inland plate boundary, north of Suruga bay, Japan. Earth Monthly, 1, 570–576 (in Japanese).

Yamazaki, H., 1992. Tectonics of a plate collision along the northern margin of the Izu peninsula, central Japan. Bull. Geol. Surv. Japan 43, 603–657.

Yamazaki, H., Shimokawa, K., Mizuno, K., Tanaka, T., 2002. Off-fault Paleoseismology in Japan: with special reference to the Fujikawa-kako fault zone, central Japan. Geographical report of Tokyo Metropolitan University. 37, 1–14.

Yamazaki, T., Seno, T., 2005. High strain rate zone in central Honshu resulting from the viscosity heterogeneities in the crust and mantle. Earth and Planetary Science Letters 232, 13–27.

Yeats, R.S., Sieh, K., Allen, C.R., 1997. The Geology of Earthquake. Oxford University Press, 557 pp.

Figure captions

Figure 1. Index maps of the study area. (a) Tectonic setting. Plate movement rates (with respect to Eurasian Plate) are cited from the Japan Meteorological Agency (2011). (b) Color shaded-relief map showing a perspective view of the study area, as generated by DEM data (1/25.000 topographic maps). (c) Topographic profile across the FKFZ and KMFZ (using DEM data). MTL: Median Tectonic Line. ISTL: Itoigawa–Shizuoka Tectonic Line. KMFZ: Kozu–Matsuda Fault Zone.

Figure 2. (a) Color relief map showing the topographic features of the study area around Mt. Fuji. (b) Geological map showing the distribution of active faults. Vertical axis is exaggerated by 10 times in scale. Straitigraphic data are cited from Tsuya (1968), Miyachi et al. (1992), and Geological Survey of Japan (2002).

Figure 3. (a) Color relief topographic map and (b) geological map showing the topographic features and distribution of active faults in the region around the southern segment of the FKFZ. (a) Vertical axis is exaggerated by 10 times in scale. Hn-hill:

Habuna Hill; Hy-hill: Hoshiyama Hill. (c)–(e) Topographical profiles across the fault scarps to show the vertical offsets of the Hoshiyama Hill (using DEM data). (d): Geological section showing the offset of the Old stage lava and Pleistocene sediments [Geological data from Yamazaki (1992)]. Locs. 1-2: location of fault outcrops shown in Figs 4-5. I.F.: Iriyama Fault. Omiya F.: Omiya Fault. Iwamoto F.: Iwamoto Fault. H: Vertical offset that is calculated from the elevations of the topographical surfaces in both sides bounded with the scarp.

Figure 4. Photographs of the Iwamoto Fault at Loc. 1 (see Fig.3b for detail location). (a) Overview of the fault outcrop. For scale, two persons are standing in the central-lower of the photograph (indicated by an white open circle). (b) Striations and fault steps on the main fault plane shown in (c). The red magic ink pen shown in the top left side is ~1.5 in diameter. (c) The fault separates unconsolidated sand–gravel layers from mudstone. Grid interval is 50 cm. (d) Sketch of (c). Note that sand veins, formed during liquefaction, were injected into the mudstone. (e) Equal-area stereographic projection showing the

orientations of striations on the main fault shown in (b). Contour interval is 5% per 1% area.

Figure 5. Photographs of the Omiya Fault at Loc. 2 (see Fig.3b for detail location). (a) Flexural fold structures developed on Hoshiyama Hill on the west side of the Omiya Fault. (b) Scarp of the Omiya Fault where the fault is cut by the New Tomei Highway. (c) Close-up view of (b).

Figure 6. (a) Color relief topographic map and (b) geological map showing the topographic features and distribution of active faults in the central segment of the FKFZ. Vertical axis is exaggerated by 10 times in scale. SK-hill: Shibakawa hill; Hn-Habuna hill (c)–(f) Topographical profiles across the fault scarps show the vertical offsets of the active faults (using DEM data). Locs 3–8: locations of fault outcrops shown in Figs 8–13. F: fault. H: Vertical offset that is calculated from the elevations of the topographical surfaces in both sides bounded with the scarp.

Figure 7. (a) Color relief map showing the topographic features of the faults in the area

around Locs 4-6. Vertical axis is exaggerated by 5 times in scale. (b) Photograph showing the scarp of the Kubo Fault where a trench was excavated at Loc. 5 (see Fig. 11). Figure 8. (a) Photograph and (b) corresponding sketch showing the structures of the Shibakawa Fault at Loc. 3 (see Fig. 6 for detail location). The tape measure shown for scale is 2 m in length. Note that the Holocene deposits are cut by faults (F1–F3), and that the sand veins caused by liquefaction occur in the medium-grained sand layer in the lower part of the exposure. FK-10, 11, 13: ^{14}C dating sample numbers (see Table 1).

Figure 9. (a, b) Photographs that give an overview of the trench site on Shibakawa Fault at Loc. 4, and (c, d), sketches of the exposed walls of trench 1(see Figs 5-6 for detail location). Note that the strata, including the humic soil layer of 439–1150 AD within the wedge vein, are offset by the fault (F). H1m: fault scarp height.

Figure 10. (a, b) Photographs and (c, d) corresponding sketches showing the exposed walls of trench 2 on the Shibakawa Fault at Loc. 4 (see Figs 5-6 for detail location). Note that the strata, including the humic soil layer of 1288–1436 AD, are offset by the fault (F),

as observed in trench 1 and shown in Fig. 9.

Figure 11. (a) Photograph and (b) corresponding sketch showing the exposed wall of the Kubo Fault at Loc. 5 (see Figs 5-7 for detail location). Note that the strata are offset by the fault. Liquefaction structures can be seen in the humic soil layer. The loam layer overlying the Shibakawa lava is offset by more than 8 m along the fault plane, whereas the scarp itself has a height of ~1.3 m.

Figure 12. (a) Photograph and (b, c) sketches showing the exposed walls of the Kubo Fault at Loc. 6 where Jomon-period archeological relics were found (see Figs 5-6 for detail location). The exposure wall of (b) is outcropped in a site 20 m far from the site of (a). Note that all the strata (875 AD to BC 1895) have been cut and offset by the faults (F1–F6).

Figure 13. (a) Photograph and (b) corresponding sketch showing the exposed wall of the Saori Fault at Loc. 7. The tape measure shown for scale is 2 m in length. Note that the Ko–Fuji mudflow (23,340 yr B.P.) and overlying deposits have been displaced by the

fault.

Figure 14. Construction site (Loc. 8) where the Kamiide Fault was exposed. (a, b) Photographs showing the scarp of the fault, and (c, d) the exposed wall of the fault. (e) Sketch of the view shown in (d). Note that west side is uplifted and the boundary between the lava and the underlying mudflow (a, b) is tilted to the east, as opposed to the general westwards slope of Mt. Fuji at this site. The alluvial layers, including volcanic ash material (scoria and pumice), yielded ^{14}C ages of 686 AD to BC 2380, and they are displaced by the fault (d, e).

Figure 15. (a) Color relief topographic map and (b) geological map showing the topographic features and location of the Omuroyama Fault in the northern segment of the FKFZ. Vertical axis is exaggerated by 15 times in scale. (c)–(d) Topographical profiles showing the vertical offsets of the active faults (using DEM data). H: Vertical offset that is calculated from the elevations of the topographical surfaces in both sides bounded with the scarp. (c)–(d) In-site measured topographical profiles showing the vertical offsets of

the active faults. Note that the Old stage lava has been offset vertically by ~55 m, whereas the 864-865 AD Jogan lava has only been displaced vertically by 2.5–3.0 m (e–f).

Figure 16. Photographs showing the scarp of the Omuroyama Fault. (a) Scarp on the Older stage lava near topographic profile H–H' shown on Fig. 15. (b) Scarp on the 864 AD Jogan lava near profile K–K' (Loc. 9), shown on Fig. 15. For scale, a person is standing in the right upper side.

Table 1. Result of the ^{14}C dating.

sample no.	lab no.	material	^{14}C age (yr BP)	Calender year (2σ)
FK-1	Beta-169585	organic soil	620±70	AD 1,288 - AD 1,436
FK-2	Beta-169584	organic soil	1,470±60	AD 439 - AD 688
FK-3	Beta-169583	organic soil	1,120±70	AD 724 - AD 1,150
FK-4	Beta-169586	organic soil	1,550±60	AD 436 - AD 662
FK-5	Beta-169587	organic soil	3,660±50	BC 2,134 - BC 1,775
FK-6	Beta-180889	organic soil	1,340±60	AD 615 - AD 785
FK-7	Beta-180890	organic soil	2,840±60	BC 1,190 - BC 840
FK-8	Beta-180891	organic ssoil	3,410±70	BC 1,895 - BC 1,525
FK-9	Beta-180892	organic soil	1,300±60	AD 640 - AD 875
FK-10	Beta-180893	organic soil	5,381±42	BC 4,337 - BC 4,216
FK-11	Beta-180894	organic soil	9,488±60	BC 8,920 - BC 8,627
FK-12	Beta-180895	wood	23,340±110	
FK-13	Beta-180898	organic soil	7,624±51	BC 6,591 - BC 6,413
C01	20111218-C01	organic soil	2,110±30	BC 172 - BC 92
C02	20111218-C02	organic soil	3,860±30	BC 2,350 - BC 2.286
C03	20111218-C03	organic soil	1,350±20	AD 653 - AD 672
C04	20111218-C04	organic soil	3,300±30	BC 1,636 - BC 1,505
C06	20111218-C06	organic soil	1,540±20	AD 432 - AD 573
C07	20111218-C07	organic soil	1,820±20	AD 130 - AD 246

*Samples were analyzed at Beta Analytic Inc. USA (sample nos. FK-1~FK13) and the Institute of Accelerator Analysis Ltd., Japan (sample nos. C01-C04) via accelerator mass spectrometry (AMS). Bulk soil was measured. Wood sample (sample no. FK-12) was taken from the Ko-Fuji mudflow.

†Radiocarbon ages were measured using accelerator mass spectrometry referenced to the year AD 1950. Analytical uncertainties are reported at 2σ.

‡Dendrochronologically calibrated calendar age by Method A from CALIB Radiocarbon Calibration Version 6.1 (Stuiver et al., 2003).

Figure1

Click here to download high resolution image

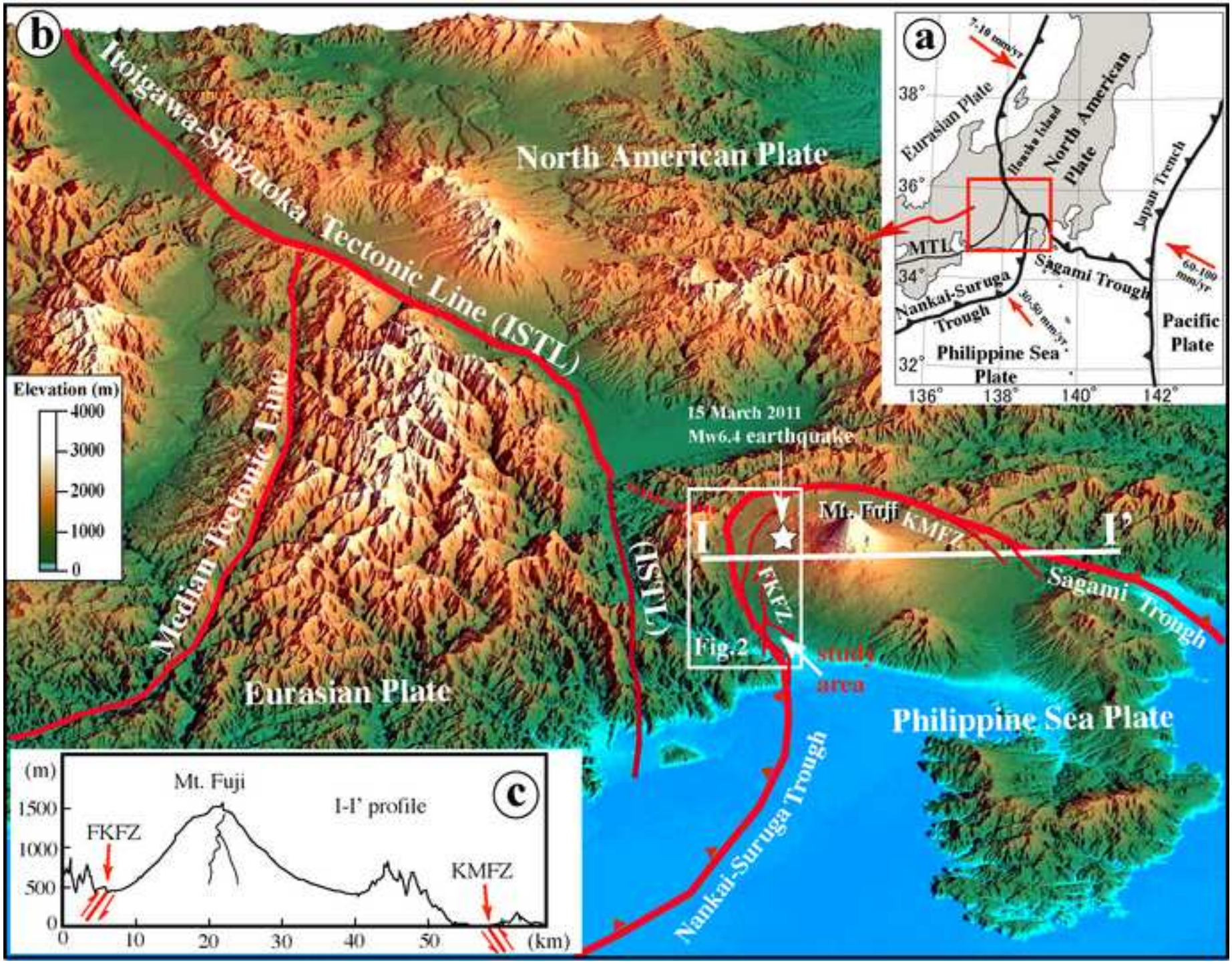

Figure2

Click here to download high resolution image

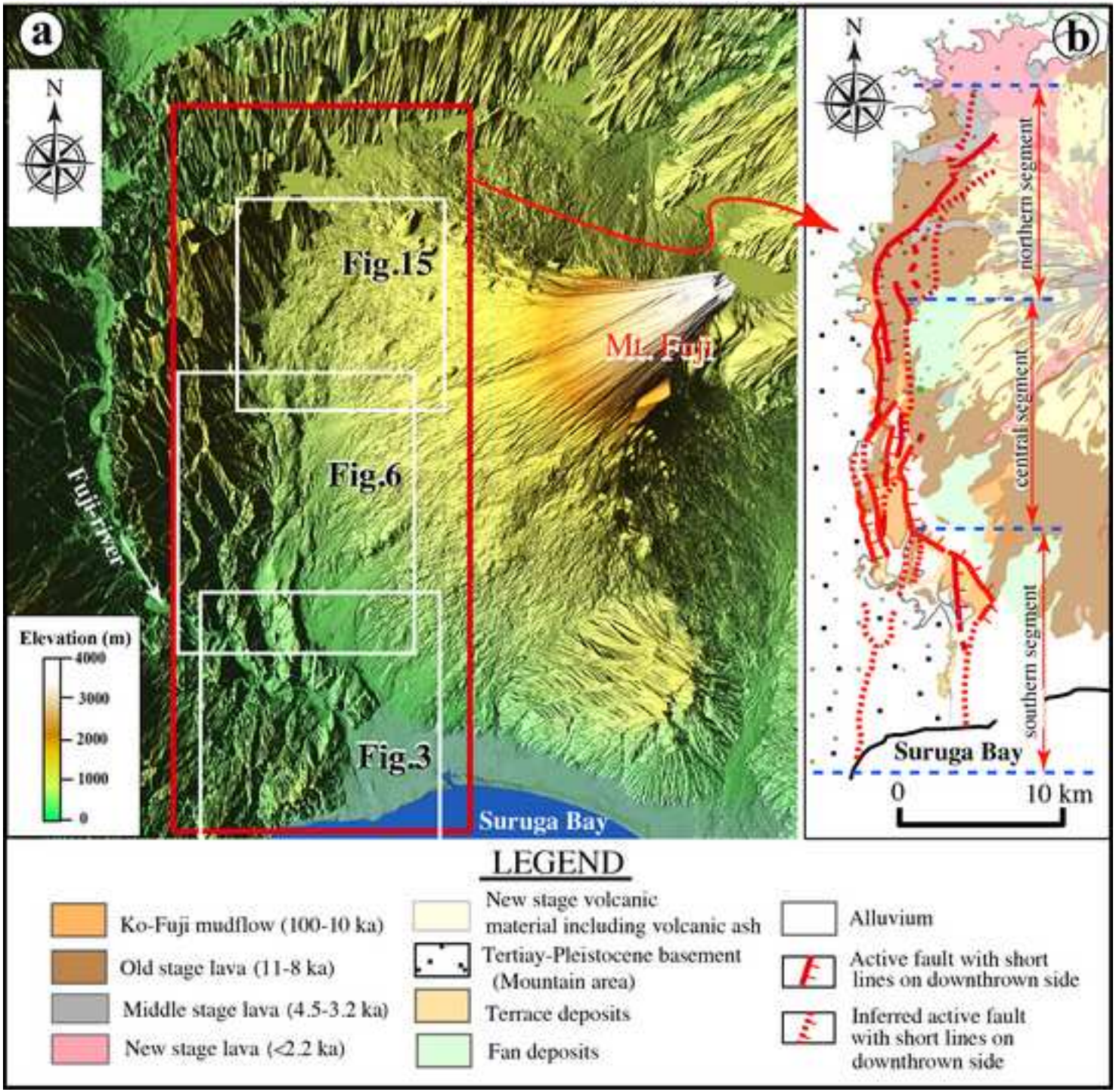

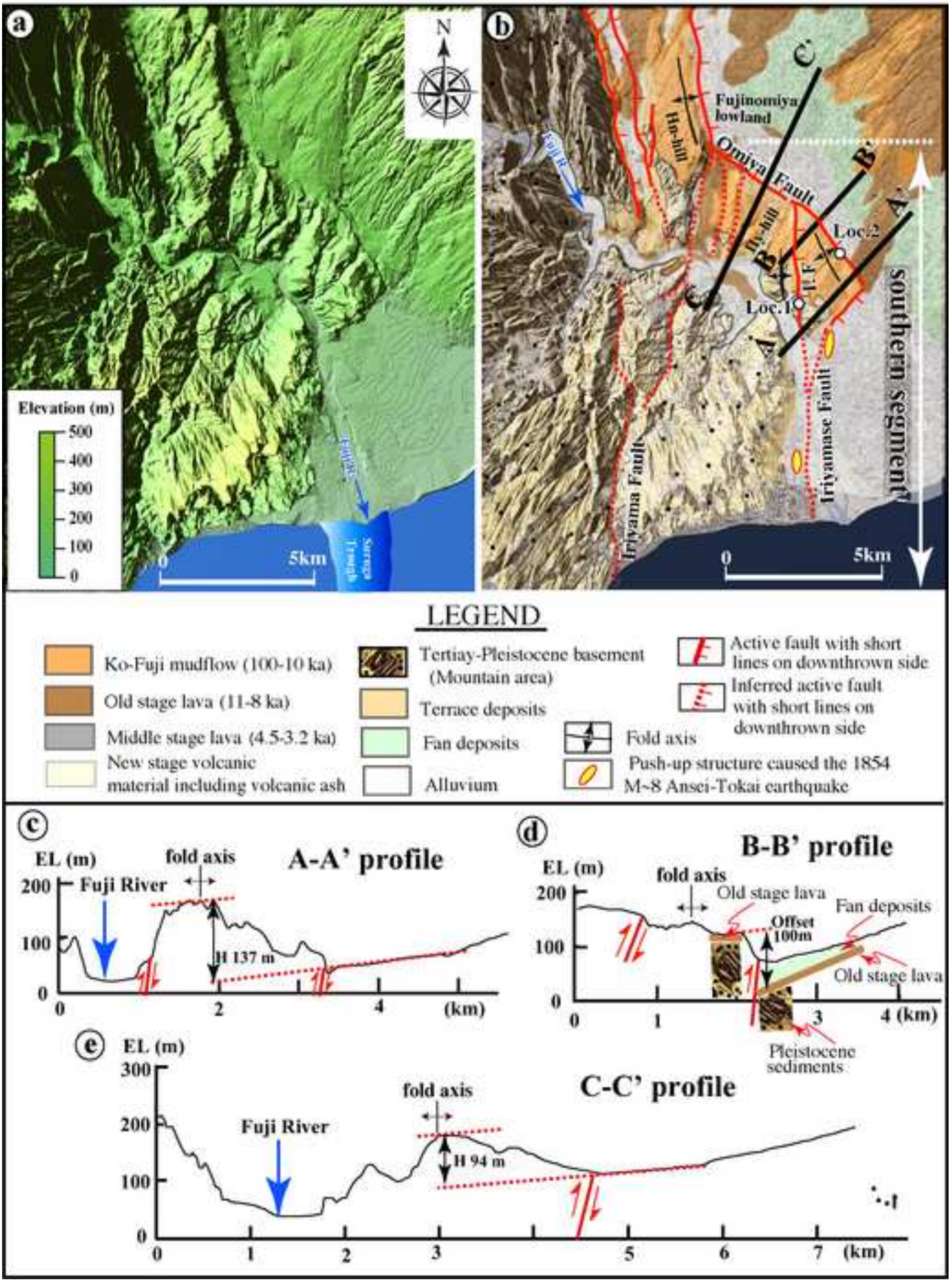

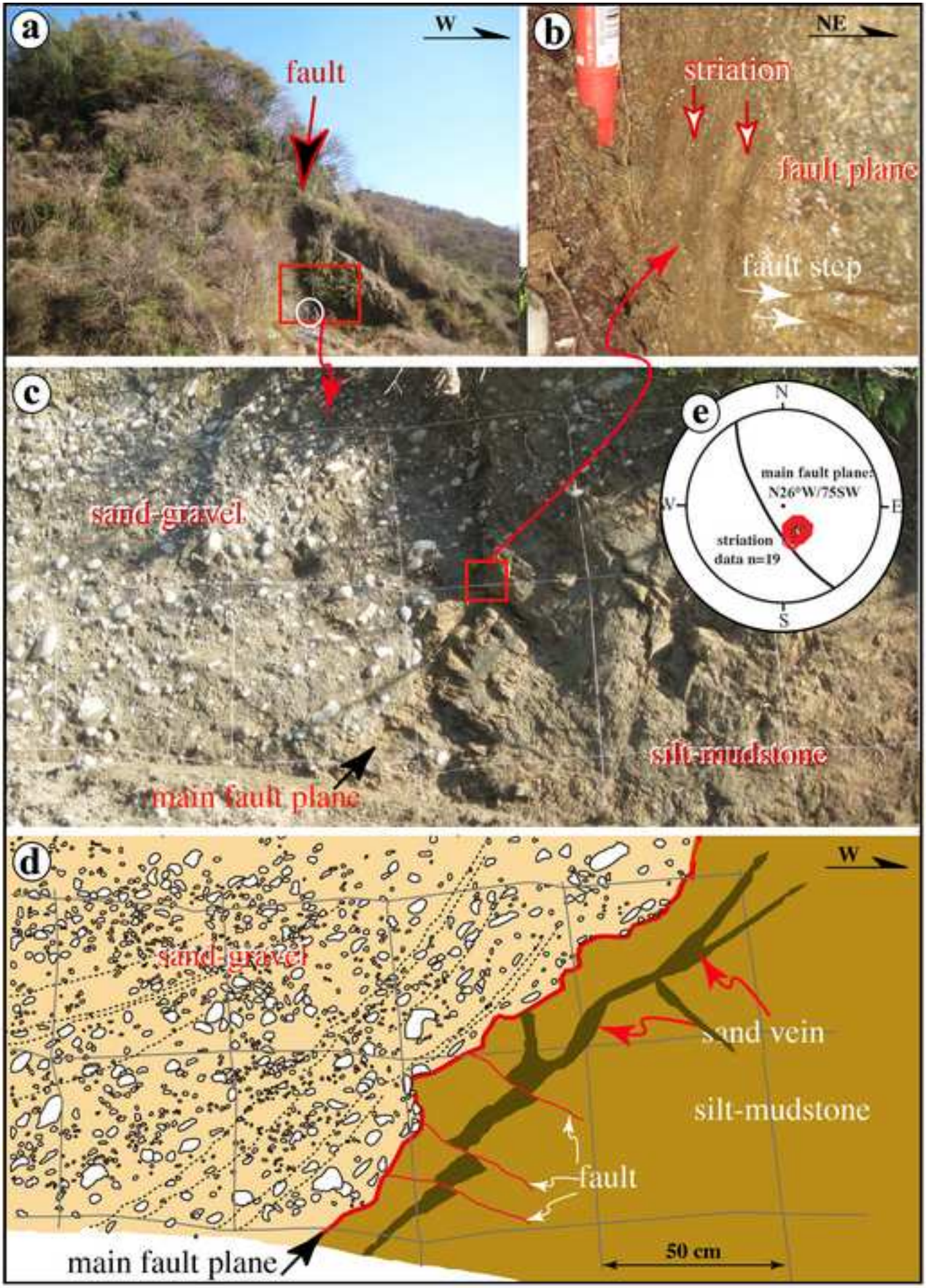

Figure5

Click here to download high resolution image

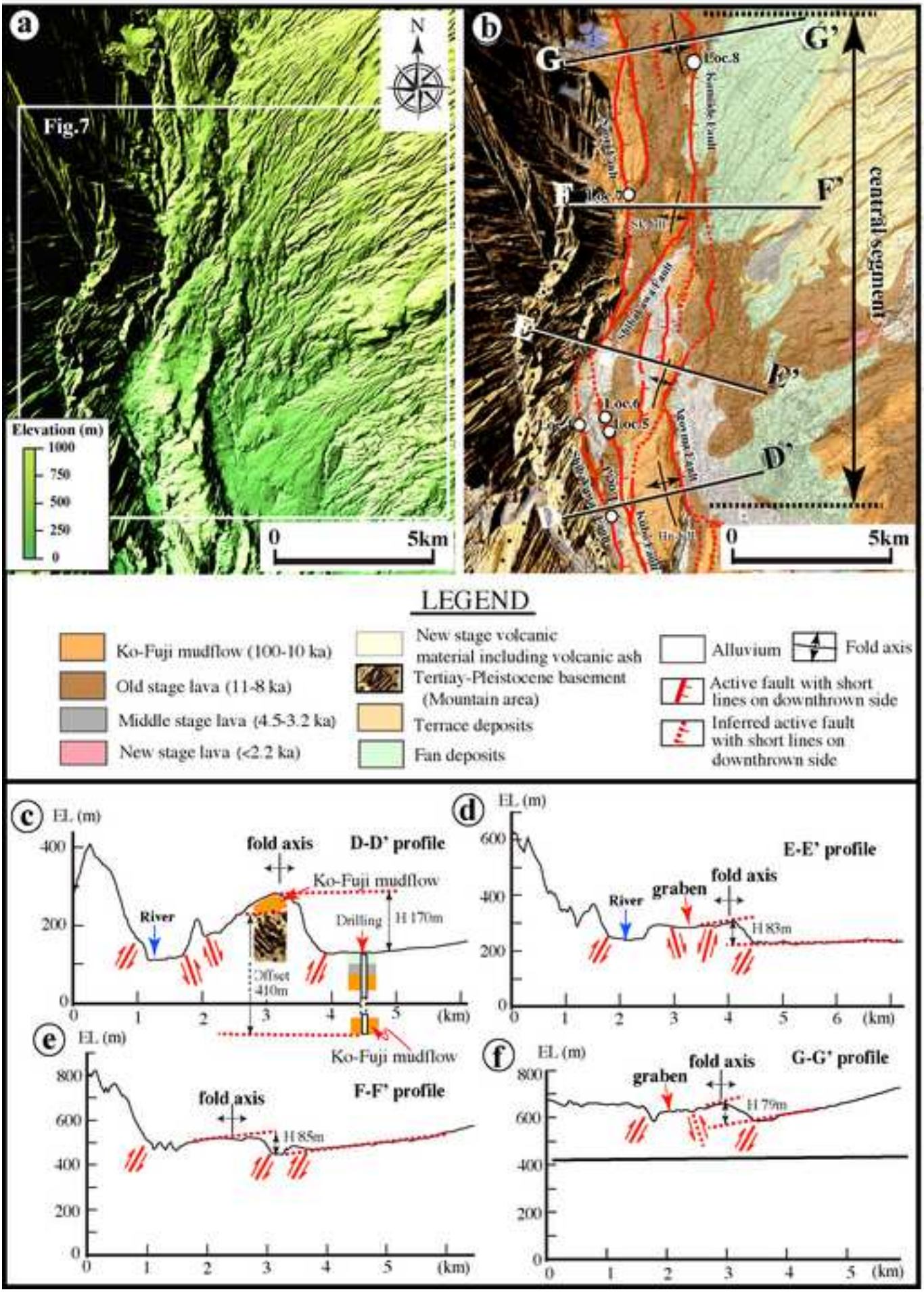

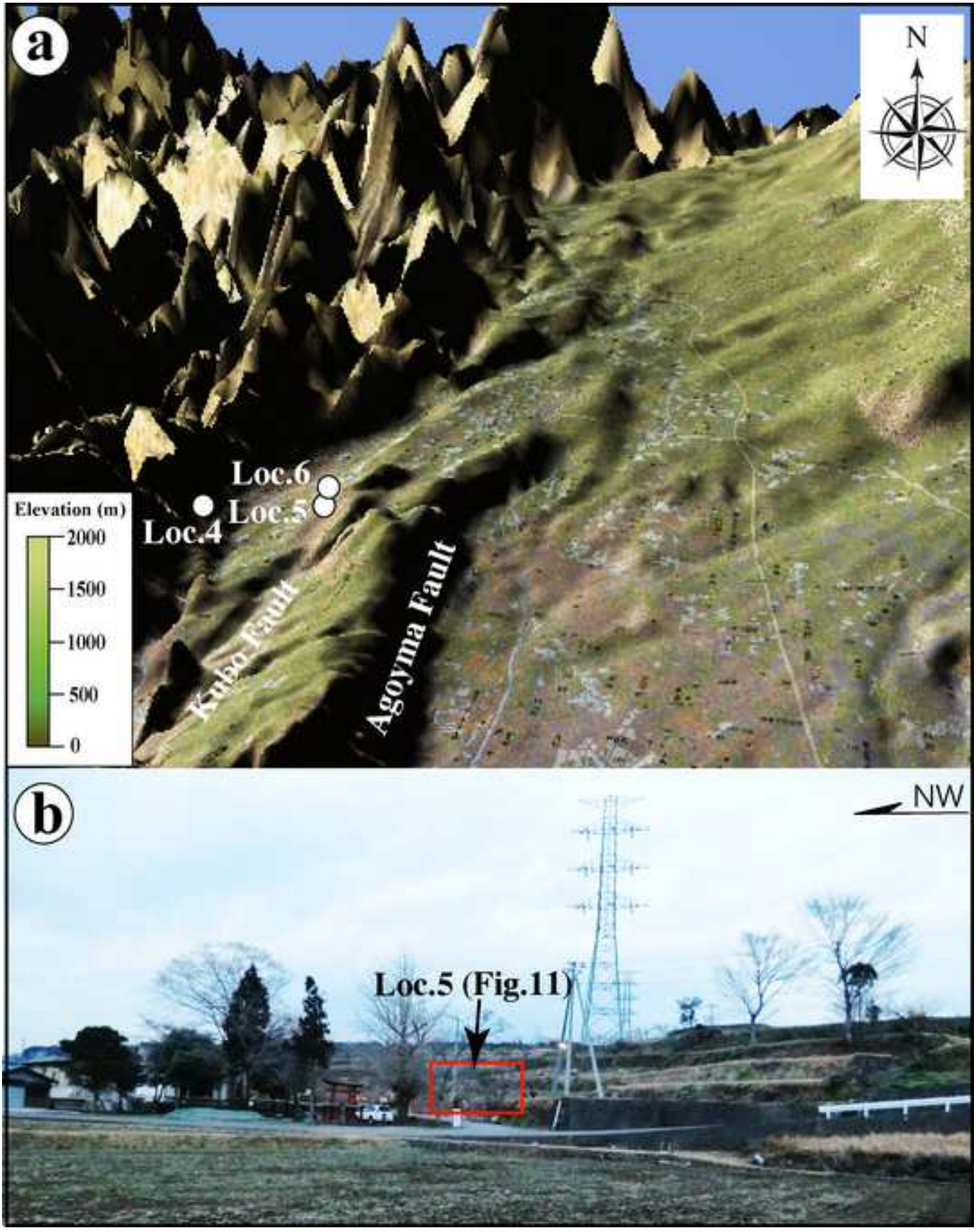

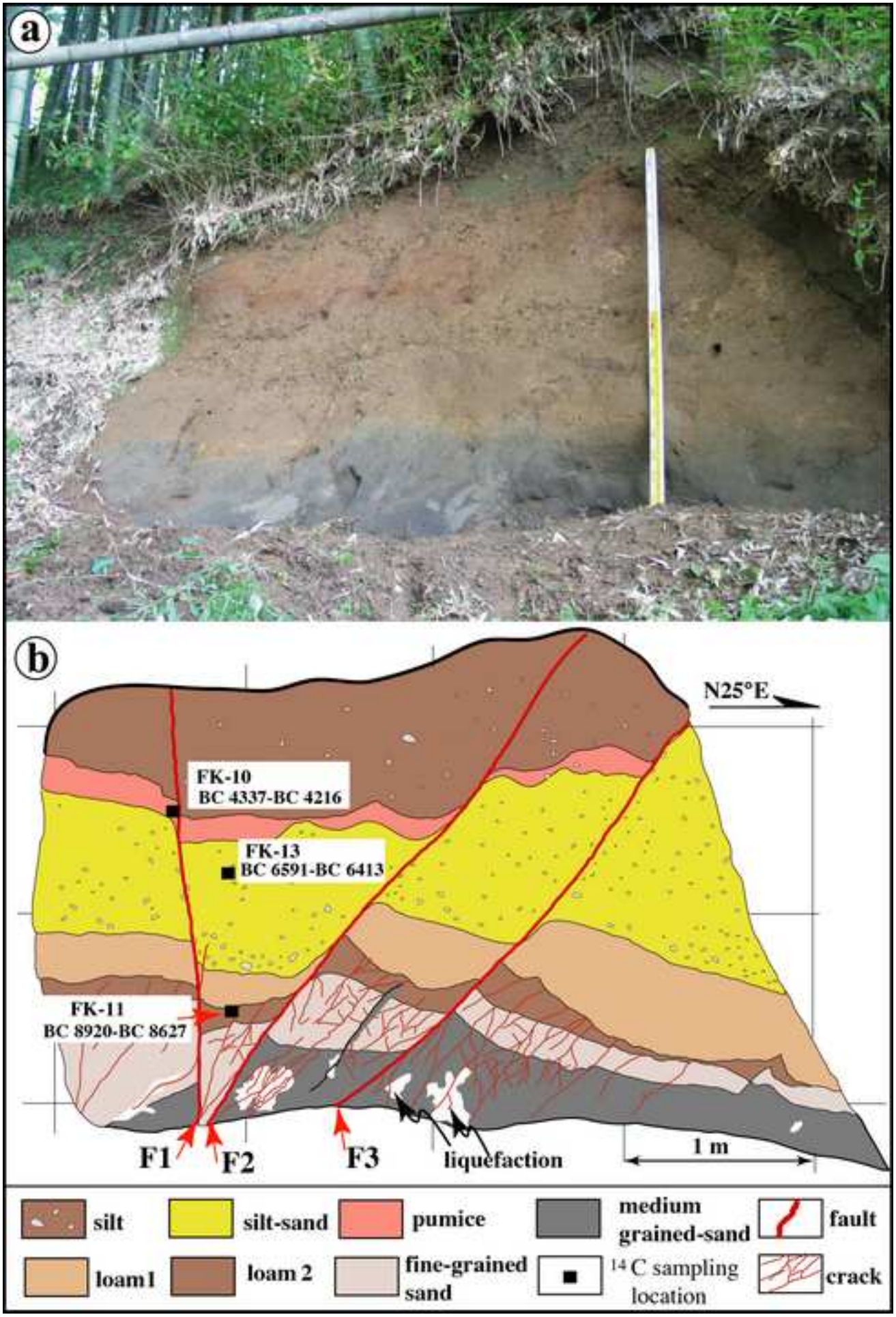

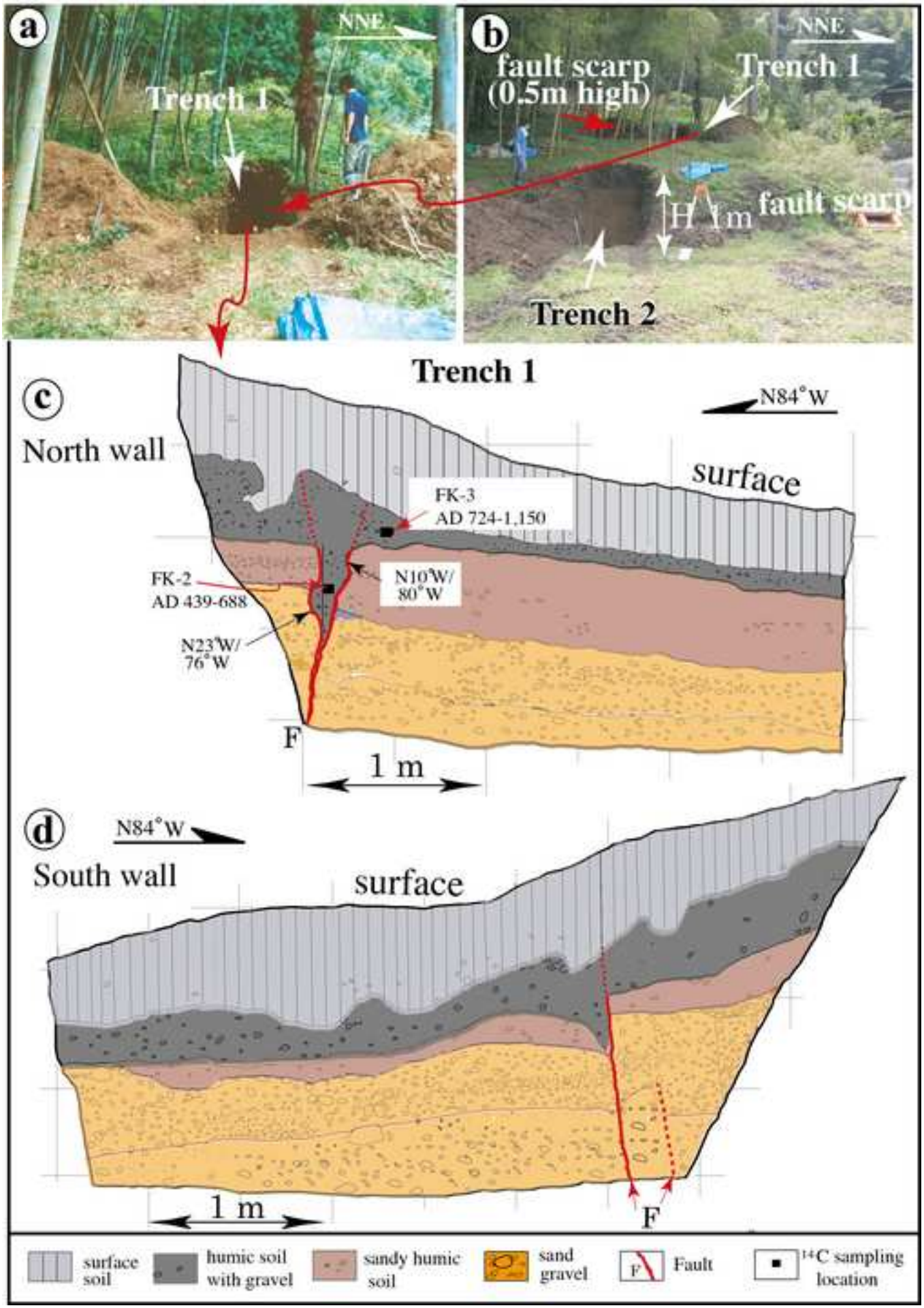

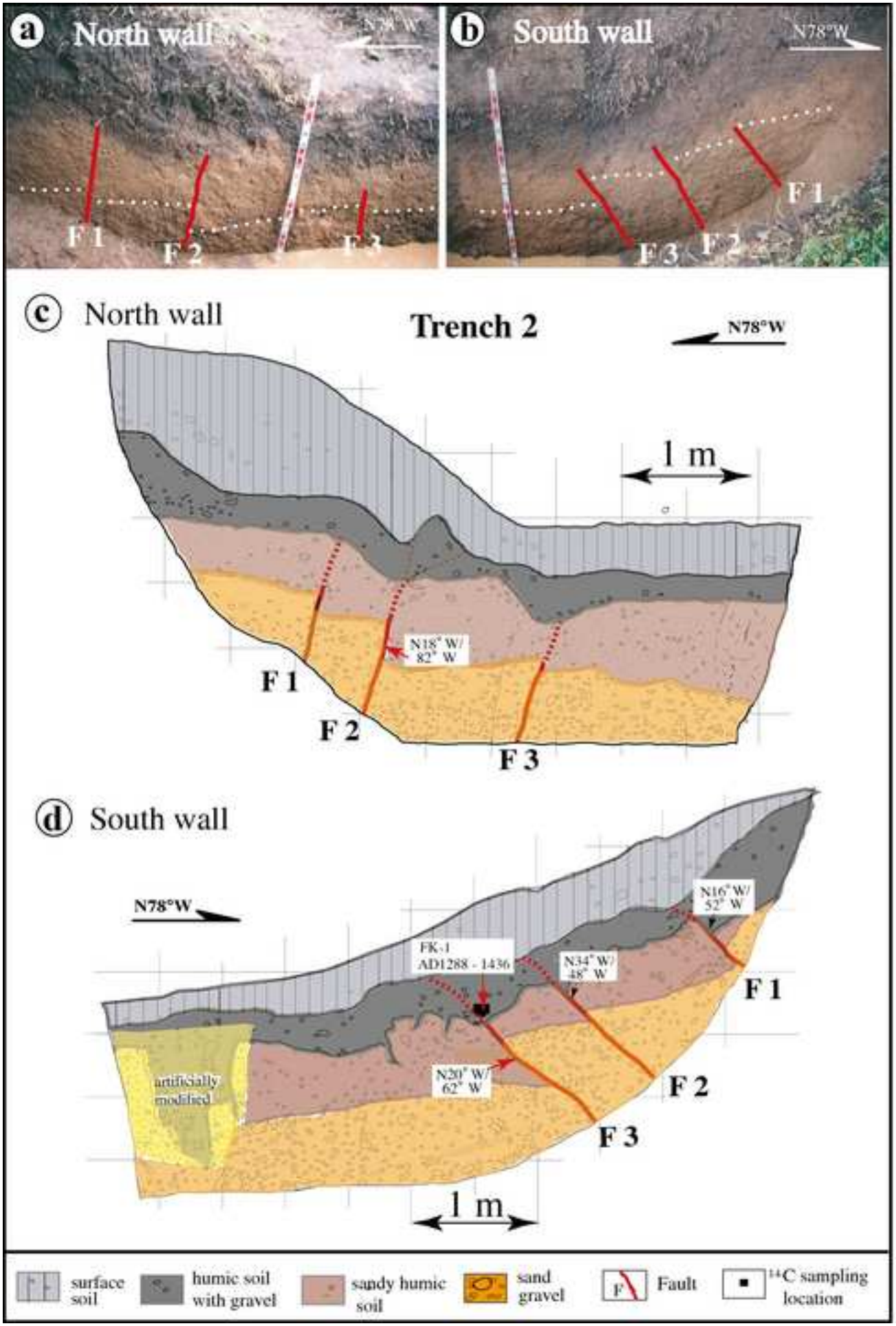

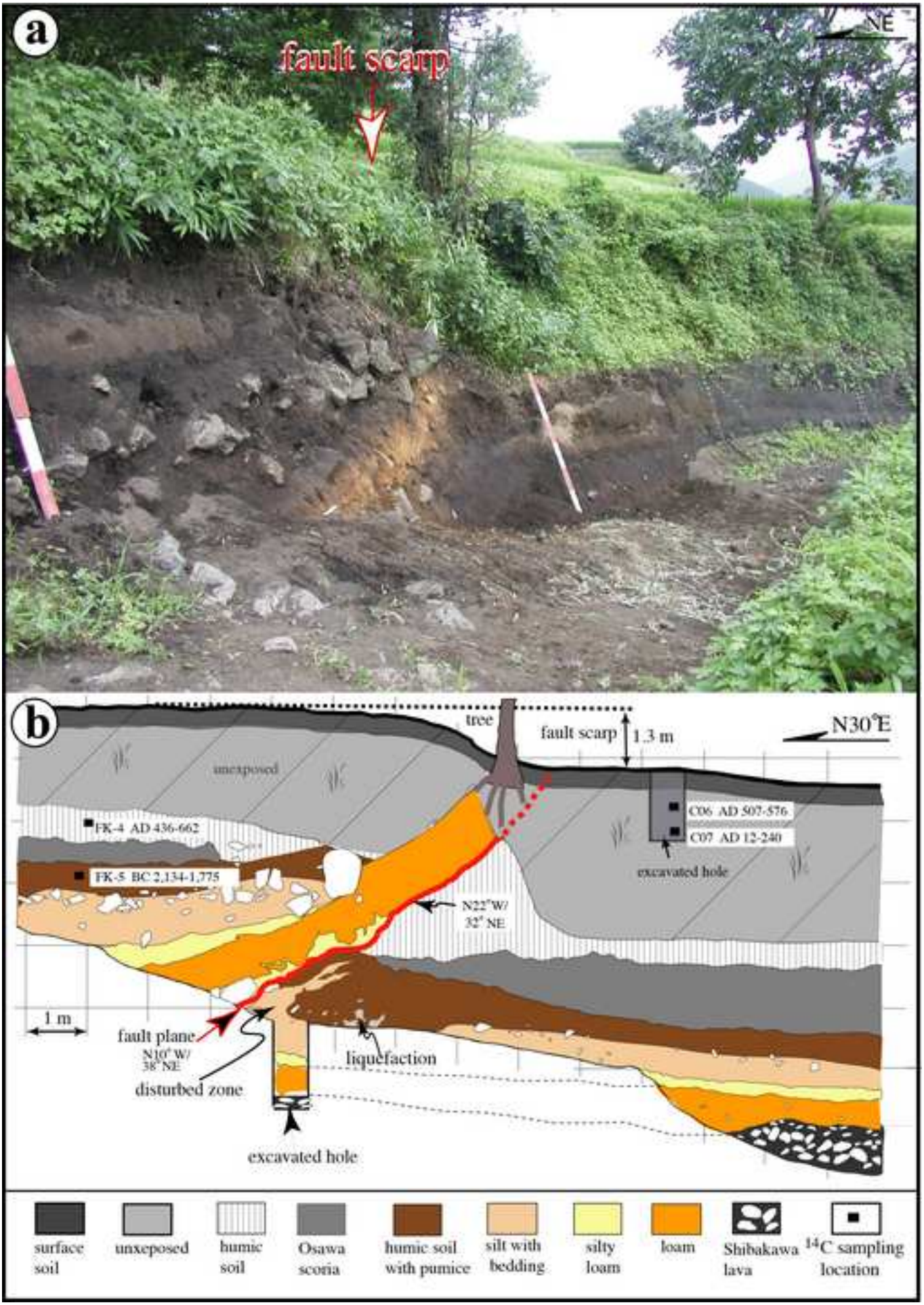

Figure12

Click here to download high resolution image